Contributions of feedforward and feedback control in a manual trajectory-tracking task

Momona Yamagami * **Darrin Howell** * **Eatai Roth** **
Samuel A. Burden *

* *Department of Electrical Engineering, University of Washington, Seattle, WA 98105 USA (e-mail:* {my13,dbhowell,sburden}@uw.edu*).*
** *Department of Intelligent Systems Engineering, Indiana University, Bloomington, IN 47405 USA (e-mail:* eatai@iu.edu*).*

Abstract: In joint human-cyber-physical systems, the human operator may rely on a combination of reactive (feedback) and predictive (feedforward) control. This paper proposes an experimental and analytical approach to simultaneously identify the human feedback and feedforward controllers in the context of human-cyber-physical systems (HCPS). In our experiments, participants play a 1DOF reference-tracking video game, tasked to guide a cursor to follow a pseudo-random trajectory. For such tasks, the model inversion hypothesis suggests that the human operator would implement as a feedforward controller the inverse of the cyber-physical-system dynamics. Our results indicate that at lower frequencies (≤ 0.15 Hz), individuals capably invert the system dynamics to implement a feedforward controller, but at higher frequencies, the magnitudes of the estimated feedforward transformation are approximately half those of the exact model inverse. This suggests that a frequency limit at which individuals are unable to follow the system dynamics, and thus, the model inversion prediction is only applicable at lower frequencies.

Keywords:
internal inverse model, sensorimotor learning, system identification

41 pt
0.569 in
14.5 mm

1. INTRODUCTION

From robot-assisted surgery to (semi-)autonomous driving, systems in which control is shared between humans and engineered systems—human-cyber-physical systems (HCPS)—are increasingly common. Whereas controllers in cyber-physical systems are designed (and therefore known), the emergent dynamics of the closed-loop *human*-cyber-physical system is shaped by the human operator, whose controller is not known *a priori*. Controllers implemented by human operators exhibit significant variability both between populations (e.g. novices and experts) and within an individual (e.g. performance may improve with experience and degrade with fatigue) (Abbink et al., 2012). As such, a predictive model of human controllers (or a particular human's controller) could provide an important tool for designing cyber-physical-systems tuned to perform robustly with a human in the loop.

In this work, we consider a trajectory tracking task in which a human operator learns to control a novel dynamical system, a task similar to steering a vehicle or guiding a robot remotely. Trajectory tracking tasks have long been a task paradigm for understanding how human operators control linear (or weakly nonlinear) systems; control theoretic models both explain and predict manual control of piloted aircraft (McRuer and Jex, 1967; Allen and McRuer, 1979). These models, however, were specifically designed to model regulation tasks performed by experts, and thus, may not generalize to more complex dynamical systems or novices. A similar approach could apply more broadly to pilot-vehicle systems.

In addition to feedback regulation on tracking error, research suggests that humans rely on internalized dynamical representations of their bodies and the environments with which they interact for motion planning (Shadmehr and Mussa-Ivaldi, 1994; Wolpert and Kawato, 1998) We hypothesize that this finding extends to the devices or vehicles they use. Importantly, such internal models permit *feedforward* control, allowing the human to predict the necessary inputs to produce the desired output trajectory, potentially increasing task performance and decreasing reliance on sensory feedback (Gawthrop et al., 2009, 2011; Desmurget and Grafton, 2000).

We experimentally investigate the human controller architecture from (Roth et al., 2017; Robinson et al., 2016) containing parallel feedback and feedforward pathways. Our experimental design makes possible the simultaneous estimation of concurrent feedback and feedforward transformations in terms of empirical frequency responses.

2. PROBLEM FORMULATION

2.1 Trajectory Tracking via Dynamic Model Inversion

In the laboratory, we instantiate the human-cyber-physical interaction as a single-degree-of-freedom, reference-tracking

task: a path-following video game in which the human operator is tasked with guiding a cursor, y, along a prescribed path, r (Fig. 1b). The human participant uses a 1 degree-of-freedom (1DOF) sliding joystick to modulate the input u. The cyber-physical system dynamics are prescribed by the model M, transforming human inputs into cursor motion.

We hypothesize that the human sensorimotor controller comprises parallel feedforward and feedback pathways, F and B respectively (Fig. 1a). The dynamic inverse model mathematical framework suggests that humans learn the forward model M and implement the inverse model as a feedforward controller, $F = M^{-1}$.

Previous studies have used such reference-tracking tasks to disentangle feedforward and feedback transforms towards validating the model inversion hypothesis (Roth et al., 2017; Zhang et al., 2018; Drop et al., 2012). In contrast to these studies, our prescribed trajectory r is an unpredictable, pseudo-random signal. As a result, the participant cannot simply learn a particular input sequence to achieve the task; rather, feedforward control requires the user to learn the forward model so that it may be generalized to novel reference trajectories. Further, we introduce an independent disturbance signal, d an additive perturbation of u, only correctable via feedback (Yu et al., 2014).

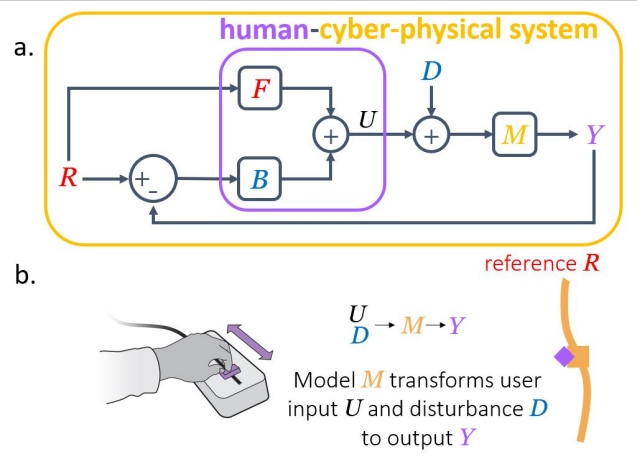

Fig. 1. a. The block diagram of HCPS highlights the feedback and feedforward human controller separation that combines to a measured user input U. Our experimental assays prescribe the reference and disturbance signals, r and d, as well as the cyber-physical model, M, and are designed to enable estimation of the distinct contributions of feedforward and feedback processes. b. A human operator completing the computer trajectory tracking task using a 1DOF slider.

Hypothesis 2.1. The user input for reference tracking with disturbance is consistent with a superposition of the responses to the reference trajectory and the disturbance signals presented individually.

2.2 Separation of Feedforward and Feedback Control Inputs

The transfer functions H_{UR} and H_{UD} map the reference and disturbance signals, respectively, to the user input. These transforms are empirically estimated for each frequency (at which we present a reference and/or disturbance) by computing the ratio of the Fourier transforms of measured signals, $\frac{U}{R}$ or $\frac{U}{D}$. We may express these empirical transforms as functions of the unknown feedforward and feedback controllers, F and B:

$$U = \underbrace{\frac{F+B}{1+BM}}_{H_{ur}} R + \underbrace{\frac{-BM}{1+BM}}_{H_{ud}} D, \tag{1}$$

$$Y = (U+D)M. \tag{2}$$

Or conversely, we estimate the feedforward and feedback controllers as functions of the empirical transforms and the prescribed system model:

$$B = \frac{-H_{ud}}{M(1+H_{ud})}, \tag{3}$$

$$F = \frac{H_{ur} + M^{-1}H_{ud}}{1+H_{ud}}. \tag{4}$$

Hypothesis 2.2. The combined feedback and feedforward model predicts user responses better than a model implementing only feedback control. The feedforward pathway is critical in modeling user responses.

3. EXPERIMENTAL METHODS

3.1 Overview of Experimental Setup

The reference and disturbance signals comprised a scaled and phase-shifted sum of sines with signal frequencies at the prime harmonics of a fundamental frequency 0.05 Hz, spanning 0.1-1.55 Hz (Fig. 2). The phase shifts were randomly chosen, and the magnitude of the sine wave at each frequency was scaled to $1/f$ for the first-order system (i.e., constant velocity), and $1/f^2$ for the second-order system (i.e., constant acceleration), such that the larger frequencies had a lower amplitude. The participants were instructed to slide a linear joystick (a 10 $k\Omega$ linear potentiometer) to modulate the input U. Each trial lasted for 40 seconds–two complete periods of the pseudorandom signal–and the user input u and output y were sampled at 60 Hz (u measured using an Arduino Due).

Table 1. Assays Presented To Human Operator

Order	1	2	3	4	5
Assay	$r+d$	d	$r+d$	r	$r+d$
# Trials	2	10	2	10	10

Three assay categories were presented to the operator: 1. only r with $d = 0$; 2. only d, with $r = 0$; and 3. $r + d$, with each at alternating frequencies such that for one frequency, either $r = 0$ or $d = 0$ (Fig. 2). For trials in which reference and disturbance signals were presented simultaneously, each signal contained alternating frequencies from the above set, even or odd components interleaved. In consecutive trials, the frequency support of r and d would be swapped. The r trajectories were displayed as a gold path having a look-ahead preview of 0.25 seconds; there was no visual representation of the disturbance, d,

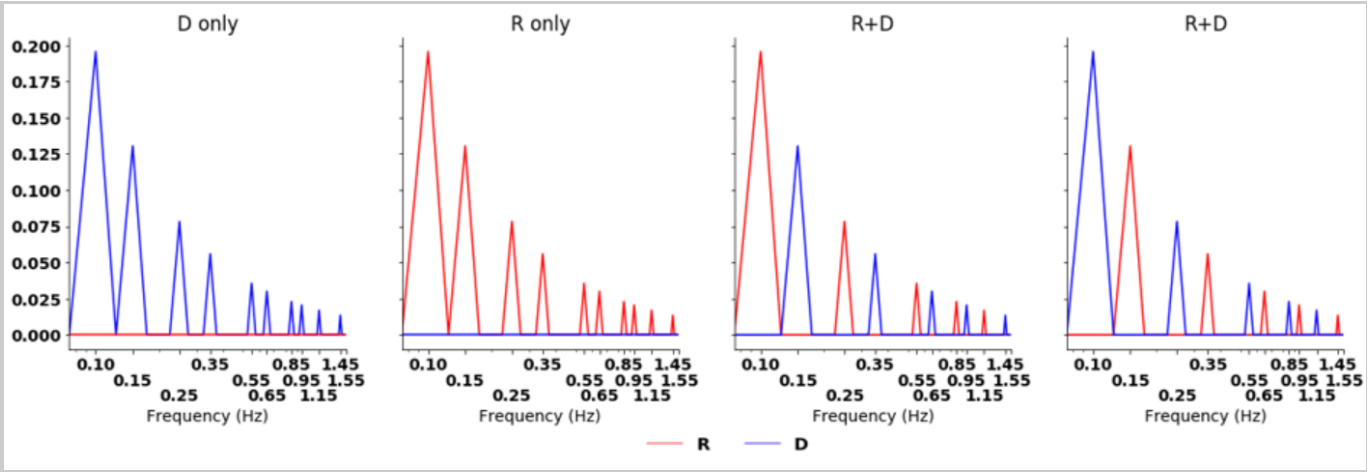

Fig. 2. The three types of assays used in the study shown as an FFT of the 40 second signal. The resolution of the axis is 0.05 Hz. The blue and red lines indicate frequency content for D and R respectively. Two types of alternating frequencies were prescribed - one where R had frequency content on the even primes and D on odd, and one where R had frequency content on the odd primes and D on even.

and consequently no look-ahead. The phase shifts for all frequency components were randomized for each trial, and the three assays were presented in sequence (Table 1).

Two models were presented sequentially to observe model inversion in a simpler first-order (FO) model and a more complex second-order (SO) model, with,

$$m_{FO} : \dot{y} = u; M_{FO} : \frac{1}{s}, \tag{5}$$

$$m_{SO} : \ddot{y} - \dot{y} = u; M_{SO} : \frac{1}{s^2 - s}. \tag{6}$$

For second order models, the spectrum of the stimuli was truncated to 0.1-0.85 Hz.

3.2 Experimental Data Analysis

Data for seven (7) participants were analyzed with Python 2.7.3. Sampled signals were converted into their frequency representations using the fast Fourier transform (FFT) Coherence was calculated in the time domain using the python function scipy.signal.coherence() between the r, d and $r + d$ trials. The Kruskal-Wallis test was conducted to determine whether the median coherence of each frequency came from the same population, and the rank sum test with a Bonferroni correction was conducted as a post-hoc test from the scipy.stats package. H_{UD} and H_{UR} in the frequency domain were also calculated to assess linearity and superposition of the HCPS. A Wilcoxon Signed-Rank test was performed to determine the extent to which the medians of H_{UD} and H_{UR} from the D, R trials were similar to the values calculated from the $R+D$ trials. The interquartile range (IQR) was calculated as a measure of spread. For all trials, circular statistics were used to unwrap the angle of the transfer functions prior to analyzing the data.

A feedback only model and a feedback and feedforward model was estimated using the D only and R only trials to determine whether the feedback and feedforward model had a better fit to the data than the feedback only model. The transfer functions were then applied to R and D in the $R+D$ trials which were not a part of the training data, and the percent error between the predicted U_p and measured U_m was calculated. The IQR of the error was calculated for both models. F and B were calculated as described in Eqns. 3, 4 to determine the extent to which F was similar to the model inverse M^{-1}. A Wilcoxon Signed-Rank test was performed to quantify this similarity.

4. RESULTS

4.1 Linearity of HCPS

The moderate coherence between the r and $r + d$ trials (median, range $C_{r,r+d} = 0.84, 0.21 - 1.0$) and d and $r + d$ trials (median, range $C_{d,r+d} = 0.82, 0.10 - 0.99$) demonstrated that $r + d$ trials may be well predicted from r and d trials by a linear least squares function (Fig. 3). This suggests that there may be a linear relationship between the system inputs r, d and the system output y. The Kruskal Wallis test demonstrated that there was a statistical difference in the medians of both H_{UR} and H_{UD} with $p < 0.001$ and $p = 0.014$ respectively. The post-hoc rank sum test indicated that there was a significant difference in the median coherence between frequencies at 0.35 Hz and lower and 1.15 Hz and higher for H_{UR}, and 0.55 Hz and lower and at 1.55 Hz for H_{UD}. This suggests that there is a lower overall coherence with increasing frequency, especially at 1.15 Hz and above, whereas there is a high coherence at 0.35 Hz and below.

Further investigation into the transfer functions H_{UR} and H_{UD} for the first-order system demonstrated a high degree of overlap between the R and $R + D$ trials and D and $R + D$ trials (Fig. 4). The Wilcoxon Signed-Rank test indicated that with $\alpha < 0.05$, there was no statistical difference in H_{UR} and H_{UD} in either average magnitude or angle between the only R or only D trials and the $R+D$ trials. Similarly to the coherence analysis, the higher frequencies tended to have a larger spread in variability across individuals for both the R only and D only trials as well as the $R + D$ trials. The positive results from this superposition test indicates that the HCPS can be thought

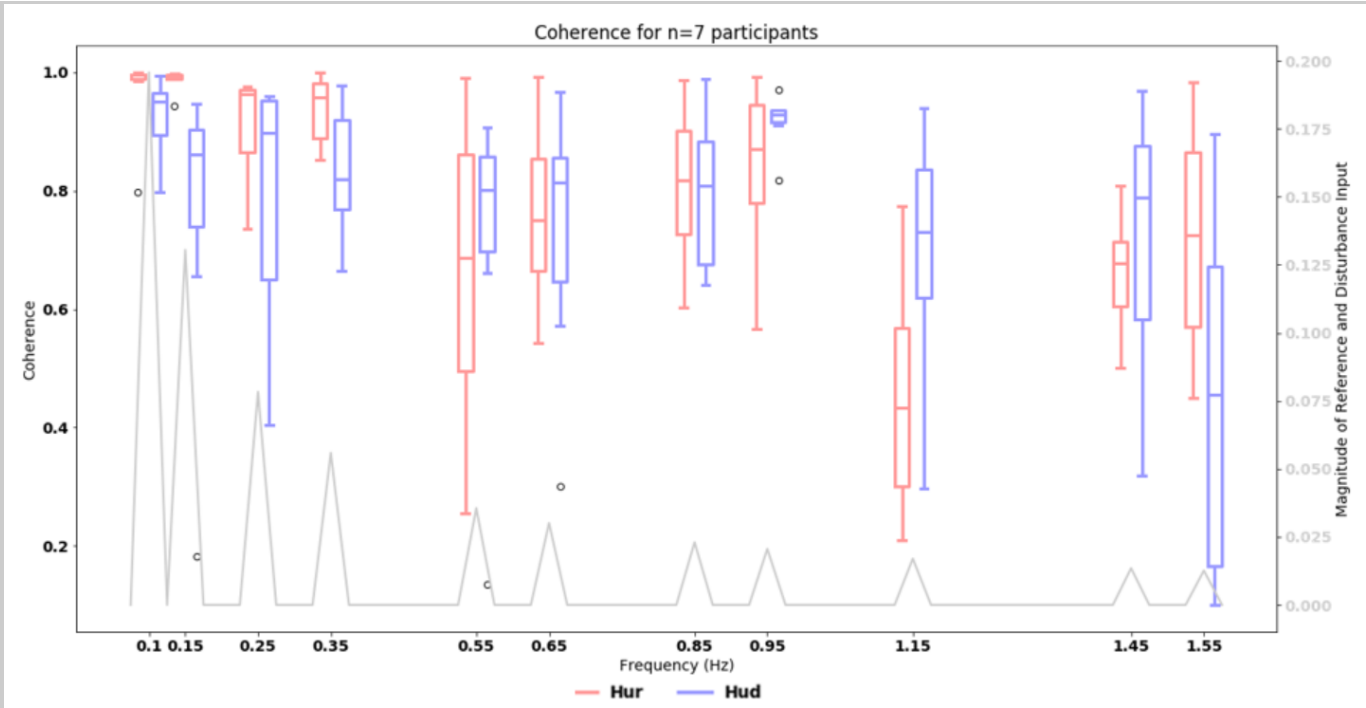

Fig. 3. Coherence values calculated between the r and d only trials and $r+d$ trials demonstrate high coherence between the two for lower frequencies, whereas the coherence at higher frequencies show a larger variability between subjects.

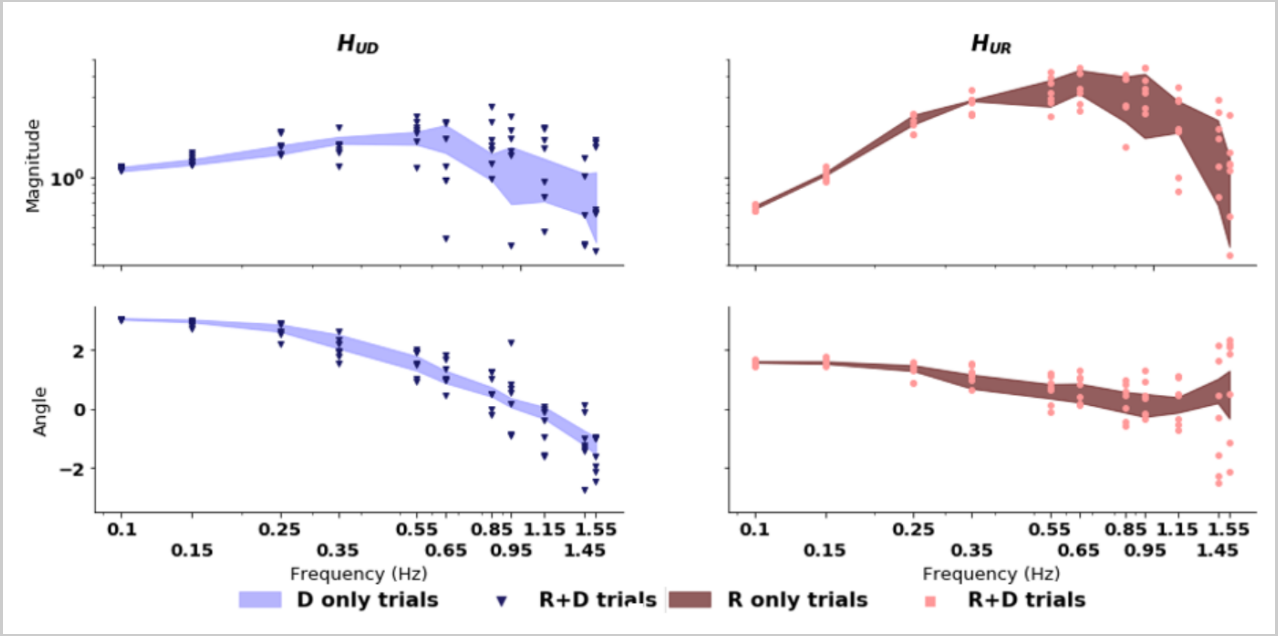

Fig. 4. Transfer functions for D to U: $H_{UD} = U/D$ and R to U: $H_{UR} = U/R$ demonstrate overlap for the transfer functions in the R and D only trials and $R+D$ trials. The shaded blue and red areas represent the IQR of H_{UD} and H_{UR} respectively from the D only and R only trials; the blue triangle represents individual H_{UD} values and the red circle represents individual H_{UR} values calculated from the $R+D$ trials.

of and analyzed as a linear system for lower frequencies below 0.35 Hz.

4.2 Feedback and Feedforward Combined Controllers Versus Feedback Only Controller

As proposed in hypothesis 2.2, human operators may control cyber-physical systems with a combination of feedforward and feedback control strategies. We verified that when a feedback only model was fitted to a subsection of the data (R only and D only trials for first-order model) and tested on a separate set of data ($R+D$ trials for first-order model), the error between the predicted U_p and measured U_m was worse than the error from the fitted feedback and feedforward model at all frequencies (Fig. 5), with the error roughly twice as high for the feedback only

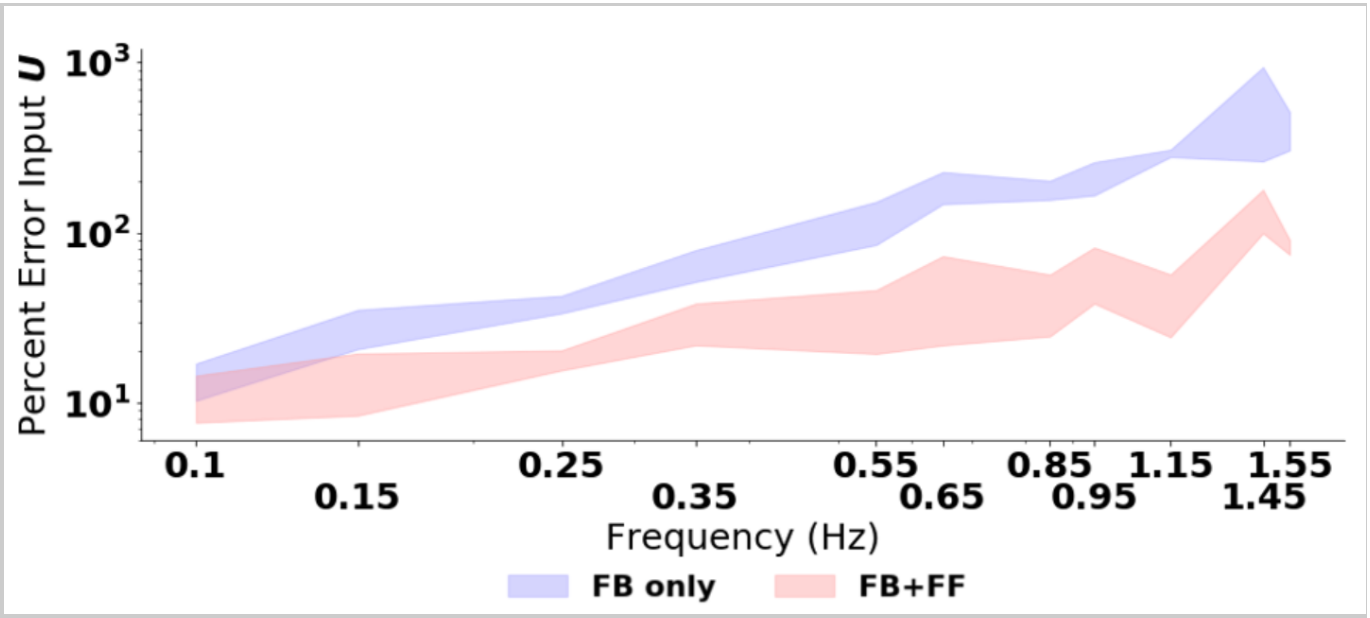

Fig. 5. The percent error between the predicted input and actual user input for the feedback only model (blue shaded area) and feedback and feedforward model (red shaded area) demonstrates lower percent error at all frequencies for the feedback and feedforward model.

model compared to the combined feedback and feedforward model. The error linearly increases in the log-log plot, suggesting that for the first-order model, the error is inversely proportional to the amplitude of the shown signal.

4.3 Dynamic Model Inversion

The feedback and feedforward estimates pooled across all individuals and trials demonstrate large deviations in magnitude from M^{-1} for the feedforward controller for both R and $R+D$ trials (Fig. 6). The Wilcoxon Signed-Rank test performed on the median F_{R+D} calculated from the $R+D$ trials for all frequencies demonstrated that there was a significant difference between the feedforward controller and M^{-1} for the magnitudes (first-order: $p = 0.006$, second-order: $p = 0.018$). The angle of the experimental feedforward block was significantly different from M^{-1} for the first order M ($p = 0.004$), but not for the second order ($p = 0.18$). Similarly, for the F calculated from the R only and D only trials, there was a significant difference in the magnitudes between the $F_{R,D}$ and M^{-1} (first-order: $p = 0.004$, second-order: $p = 0.04$) and the angle for the first-order model ($p = 0.006$), while we again failed to verify a difference in the angles for the second-order system ($p = 0.74$).

Looking more closely at whether there is a difference between the median F and expected M^{-1} magnitude at each frequency, we found that the magnitude was consistently lower than the expected M^{-1} at all frequencies except 0.1 Hz and 0.15 Hz, as demonstrated by the Wilcoxon Signed-Rank test ($p < 0.05$) for both the first and second-order system. The magnitude of the higher frequencies at 0.25 Hz and above were lower than the expected M^{-1} magnitude by a median factor of 0.54 (range: $0.43 - 0.70$) for the first-order system and a median factor of 0.59 (range: $0.41 - 0.69$) for the second-order system.

5. DISCUSSION

We estimated feedback and feedforward elements of human sensorimotor control in a trajectory tracking task. Estimates were obtained for two models ($M_{FO} = 1/S$ and $M + SO = 1/(S^2 - S)$) using two different assays; both estimates agreed to within experimental error for frequencies up to 0.15 Hz. Furthermore, including the feedforward pathway roughly halves the human input prediction error, suggesting both feedforward and feedback elements may be required to predict human control of cyber-physical systems.

In contrast to the recent results reported in (Zhang et al., 2018), the estimated feedforward transformation only agrees with the inverse of the cyber-physical system model at low frequencies at 0.15 Hz and below. At higher frequencies at 0.25 Hz and above, we demonstrated that the magnitudes are lower than the expected magnitude of M^{-1} by roughly a factor of 0.5 (Fig. 6). This was corroborated with our statistical tests, which demonstrated that with an $\alpha < 0.05$, the median for both models did not have M^{-1} as the median for either the magnitude or the angle.

This result is consistent with the coherence values calculated in Fig. 3, which demonstrated that lower frequencies at 0.35 Hz and below tended to have a higher median coherence and smaller variability than the higher frequencies, suggesting a more linear HCPS at lower frequencies than higher frequencies. The transfer functions for H_{UD} and H_{UR} had similar results where frequencies larger than 0.55 Hz tended to have a much larger variability in both magnitude and angle than the lower frequencies.

This decrease in linearity with increase in frequency may be due to a number of reasons, including the strength of the signal provided and the limits of the human visuomotor response. For this study, we chose to provide human operators with a lower signal amplitude for higher frequencies

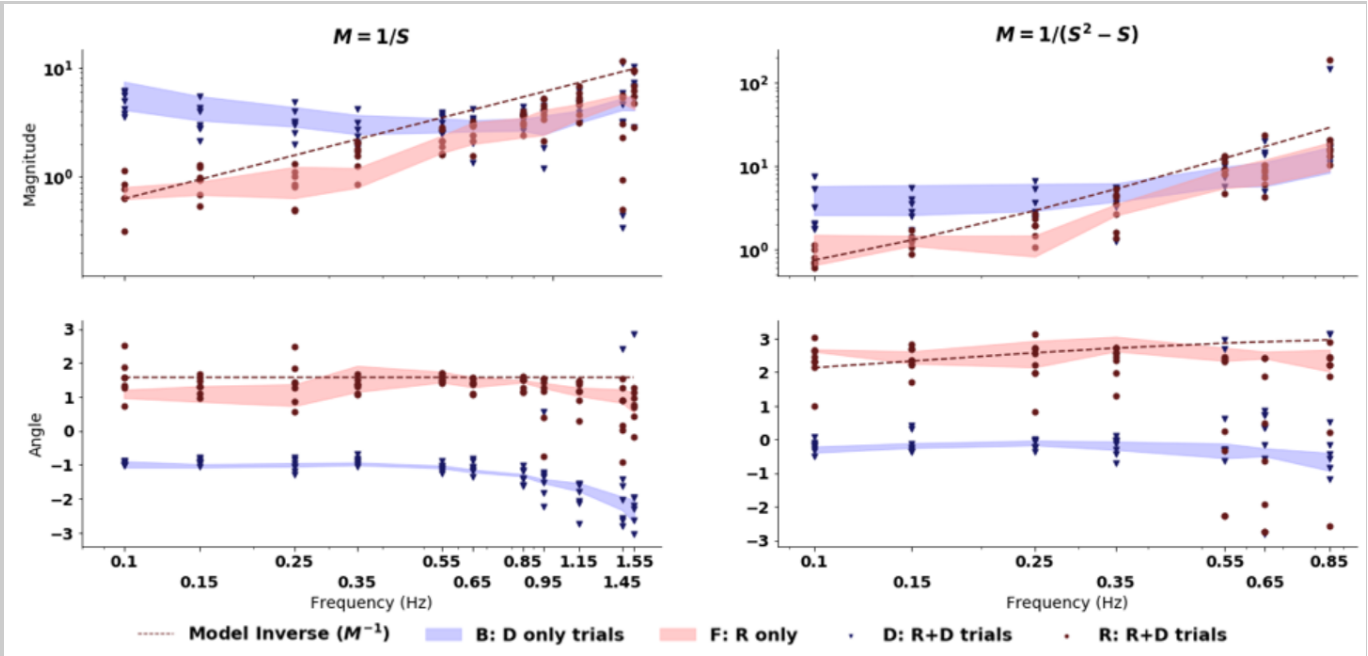

Fig. 6. The experimental values of F and B demonstrate for both first and second order closer model inversion for lower frequencies than higher frequencies in magnitude. The red dotted line represents the model inverse, the shaded red and blue is the IQR for F and B calculated from R only and D only trials, and the dark blue triangle and dark red circle represents F and B calculated from $R + D$ trials for each individual. For higher frequencies, the magnitude is consistently lower than the expected magnitude from M^{-1}

.

inversely proportional to the frequency for first-order, and inversely proportional to the square of the frequency for the second-order system, which will magnify any errors that the human operator makes while tracking these higher frequencies. Another possible explanation is human visuomotor limitations which suggests that the fastest motor reaction time for humans (as demonstrated by asking a human subject to press a button upon the presentation of a certain visual) is about 5 Hz (Wardle, 1998).

While the feedback and feedforward model can do no worse than the feedback only model in predicting the output of the training dataset, the increased number of variables in the feedback and feedforward model may lead to overfitting and thus, large errors in the validation dataset. Using the final $R + D$ trials as a validation set, we confirmed that the combined feedback and feedforward model had less error predicting the user response at all frequencies as compared to the feedback-only model. This result suggests that we did not overfit, and in fact, both the feedforward and feedback controllers lead to a better model of the HCPS.

6. CONCLUSION

This paper proposes a novel experiment design that enables estimation of human feedback and feedforward transformations in trajectory tracking tasks directly from empirical frequency responses to reference and disturbance inputs. Our results support the hypothesis that humans learn to use the inverse of the cyber-physical system model in their feedforward control pathway only at frequencies at 0.15 Hz and below, and the estimated feedforward transformation for higher frequencies resembles a scaled-down version of the model inverse. Further investigations are needed to characterize the feedforward transformations learned by human operators.

41 pt
0.569 in
14.5 mm

ACKNOWLEDGEMENTS

This research is supported by a grant from the National Science Foundation under the CISE CRII CPS (Award # 1565529), the Air Force Office of Scientific Research under grant FA9550-14-1-0398, and the Washington Research Foundation Funds for Innovation in Neuroengineering.

REFERENCES

Abbink, D.A., Mulder, M., and Boer, E.R. (2012). Haptic shared control: smoothly shifting control authority? *Cognition, Technology & Work*, 14(1), 19–28.

Allen, R.W. and McRuer, D. (1979). The man/machine control interface pursuit control. *Automatica*, 15(6), 683–686.

Desmurget, M. and Grafton, S. (2000). Forward modeling allows feedback control for fast reaching movements. *Trends in cognitive sciences*, 4(11), 423–431.

Drop, F.M., Pool, D.M., Damveld, H.J., van Paassen, M.M., Bülthoff, H.H., and Mulder, M. (2012). Identification of the transition from compensatory to feedforward behavior in manual control. In *Systems, Man, and Cybernetics (SMC), 2012 IEEE International Conference on*, 2008–2013. IEEE.

Gawthrop, P., Loram, I., and Lakie, M. (2009). Predictive feedback in human simulated pendulum balancing. *Biological cybernetics*, 101(2), 131–146.

Gawthrop, P., Loram, I., Lakie, M., and Gollee, H. (2011). Intermittent control: A computational theory of human control. *Biological cybernetics*, 104(1-2), 31–51.

McRuer, D.T. and Jex, H.R. (1967). A review of quasi-linear pilot models. *IEEE Transactions on Human Factors in Electronics*, (3), 231–249.

Robinson, R.M., Scobee, D.R., Burden, S.A., and Sastry, S.S. (2016). Dynamic inverse models in human-cyber-physical systems. In *Micro-and Nanotechnology Sensors, Systems, and Applications VIII*, volume 9836, 98361X. International Society for Optics and Photonics.

Roth, E., Howell, D., Beckwith, C., and Burden, S.A. (2017). Toward experimental validation of a model for human sensorimotor learning and control in teleoperation. In *Micro-and Nanotechnology Sensors, Systems, and Applications IX*, volume 10194, 101941X. International Society for Optics and Photonics.

Shadmehr, R. and Mussa-Ivaldi, F.A. (1994). Adaptive representation of dynamics during learning of a motor task. *Journal of Neuroscience*, 14(5), 3208–3224.

Wardle, D. (1998). The time delay in human vision. *The physics teacher*, 36(7), 442–444.

Wolpert, D.M. and Kawato, M. (1998). Multiple paired forward and inverse models for motor control. *Neural networks*, 11(7-8), 1317–1329.

Yu, B., Gillespie, R.B., Freudenberg, J.S., and Cook, J.A. (2014). Human control strategies in pursuit tracking with a disturbance input. In *Decision and Control (CDC), 2014 IEEE 53rd Annual Conference on*, 3795–3800. IEEE.

Zhang, X., Wang, S., Hoagg, J.B., and Seigler, T.M. (2018). The roles of feedback and feedforward as humans learn to control unknown dynamic systems. *IEEE transactions on cybernetics*, 48(2), 543–555.